

# SCIsegV2: A Universal Tool for Segmentation of Intramedullary Lesions in Spinal Cord Injury

Enamundram Naga Karthik<sup>\*1,2</sup>, Jan Valošek<sup>\*1,2,3</sup>, Lynn Farner<sup>4</sup>, Dario Pfyffer<sup>4,5</sup>, Simon Schading-Sassenhausen<sup>4</sup>, Anna Le Bret<sup>4</sup>, Gergely David<sup>4</sup>, Andrew C. Smith<sup>6</sup>, Kenneth A. Weber II<sup>5</sup>, Maryam Seif<sup>4,7</sup>, RHSCIR Network Imaging Group, Patrick Freund<sup>\*\*4,7</sup>, and Julien Cohen-Adad<sup>\*\*1,2,8,9</sup>

<sup>1</sup> Polytechnique Montreal, Montreal, QC, Canada

<sup>2</sup> Mila - Quebec AI Institute, Montreal, QC, Canada

<sup>3</sup> Palacký University Olomouc, Olomouc, Czechia

<sup>4</sup> University of Zürich, Zürich, Switzerland

<sup>5</sup> Stanford University School of Medicine, Stanford, California, USA

<sup>6</sup> University of Colorado School of Medicine, Aurora, Colorado, USA

<sup>7</sup> Max Planck Institute for Human Cognitive and Brain Sciences, Leipzig, Germany

<sup>8</sup> CHU Sainte-Justine, Université de Montréal, Montreal, QC, Canada

<sup>9</sup> Functional Neuroimaging Unit, CRIUGM, Université de Montréal, QC, Canada

{naga-karthik.enamundram,jan.valosek}@polymtl.ca

**Abstract.** Spinal cord injury (SCI) is a devastating incidence leading to permanent paralysis and loss of sensory-motor functions potentially resulting in the formation of lesions within the spinal cord. Imaging biomarkers obtained from magnetic resonance imaging (MRI) scans can predict the functional recovery of individuals with SCI and help choose the optimal treatment strategy. Currently, most studies employ manual quantification of these MRI-derived biomarkers, which is a subjective and tedious task. In this work, we propose (i) a universal tool for the automatic segmentation of intramedullary SCI lesions, dubbed **SCIsegV2**, and (ii) a method to automatically compute the width of the tissue bridges from the segmented lesion. Tissue bridges represent the spared spinal tissue adjacent to the lesion, which is associated with functional recovery in SCI patients. The tool was trained and validated on a heterogeneous dataset from 7 sites comprising patients from different SCI phases (acute, sub-acute, and chronic) and etiologies (traumatic SCI, ischemic SCI, and degenerative cervical myelopathy). Tissue bridges quantified automatically did not significantly differ from those computed manually, suggesting that the proposed automatic tool can be used to derive relevant MRI biomarkers. **SCIsegV2** and the automatic tissue bridges computation are open-source and available in Spinal Cord Toolbox (v6.4 and above) via the `sct_deepseg -task seg_sc_lesion_t2w_sci` and `sct_analyze_lesion` functions, respectively.

**Keywords:** Spinal Cord Injury · Segmentation · MRI · Deep Learning · Tissue Bridges

\* these authors contributed equally to this work

\*\* joint senior authors

## 1 Introduction

Traumatic and non-traumatic spinal cord injuries (SCI) represent damage to the spinal cord (SC) with severe consequences, including weakness and paralysis in patients [4]. Traumatic SCI arises from sudden physical impacts, such as car accidents or falls, while non-traumatic SCI can be caused by ischemia (ischemic SCI) or chronic mechanical compression of the SC (degenerative cervical myelopathy, DCM) [4,1]. Both traumatic and non-traumatic SCI commonly involve intramedullary lesions, which are critical areas of tissue damage within the SC. Magnetic resonance imaging (MRI) is routinely used to provide information on the extent and the location of these intramedullary lesions [4,5,22]. Importantly, MRI scans can also be used to compute quantitative biomarkers, such as midsagittal tissue bridges [8]. These help in quantifying the amount of preserved SC neural tissue (carrying motor and sensory information to and from the brain) and have been found to predict functional recovery in patients with traumatic and non-traumatic SCI [8,16,17,20,23,18].

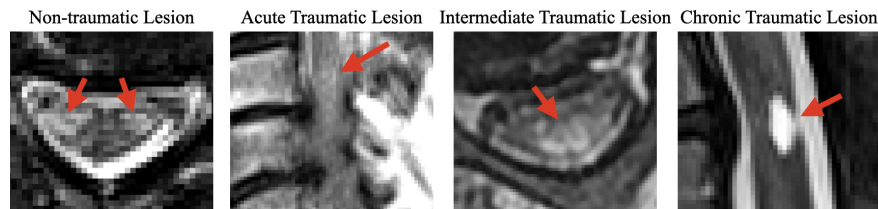


**Fig. 1.** Representative axial and sagittal T2w MRI scans of the lesion in various SCI etiologies/types.

Identifying MRI biomarkers in SCI automatically is challenging due to the varying size and location of lesions across patients and injury phases. Lesions can evolve from hyper- to hypo-intense depending on the underlying pathological mechanism (Figure 1), and metal implants in the spine often cause image artifacts [5]. As a result, most studies report biomarkers quantified from manual lesion annotations [8,24,17,19,20,16,23,18], which is a tedious and error-prone task subject to inter-rater variability, making large-scale studies impractical. While two existing studies proposed automatic lesion segmentation in SCI, their methods were developed for specific SCI etiologies: [13] focused on *acute* preoperative traumatic SCI lesions, whereas, [14] introduced `SCIseg`, an open-source model for predominantly chronic, post-operative traumatic and ischemic SCI lesions. However, maintaining multiple etiology-specific models is challenging, highlighting the need for a single, **comprehensive** model for segmenting any kind of SCI lesions. In this regard, our contributions in this work are as follows:

- **Segmentation tool:** We present a comprehensive tool for the automatic segmentation of intramedullary SCI lesions, dubbed `SCIsegV2`. Our model was trained and validated on a heterogeneous, multinational dataset from

- 7 sites consisting of (i) traumatic SCI (acute preoperative, sub-acute and chronic postoperative) and (ii) non-traumatic SCI (ischemic SCI and DCM).
- **Analysis tool:** We propose a method to automatically compute the mid-sagittal tissue bridges, a predictor of functional recovery in SCI patients.
  - **Packaging in open-source software suite:** Both SCIsegV2 and the automatic tissue bridges computation are open-source and will be integrated into the Spinal Cord Toolbox (SCT) v6.4 and higher.

## 2 Materials and Methods

### 2.1 Dataset

We used T2-weighted (T2w) MRI images with heterogeneous image resolutions (isotropic, sagittal, and axial) and magnetic field strengths (1.0T, 1.5T, and 3.0T) from seven sites. The number of patients from each site is as follows: {site 1: ( $n = 154$ ), site 2: ( $n = 80$ ), site 3: ( $n = 14$ ), site 4: ( $n = 11$ ), site 5: ( $n = 23$ ), site 6: ( $n = 4$ ), site 7: ( $n = 5$ )}. Site 1 contained patients with both traumatic ( $n = 97$ ) and non-traumatic SCI (mainly, DCM) ( $n = 57$ ). Sites 2 & 3 included both preoperative and postoperative traumatic SCI, while sites 4 to 7 included only acute preoperative traumatic SCI. The timing of the MRI examination in relation to injury for traumatic SCI patients from sites 1, 2, and 3 is detailed in Table 1 of [14]. Eight patients from site 1 were followed up with additional MRI examinations, and 40 patients from site 1 had both sagittal and axial T2w images. Patients from sites 1 & 2 were split according to 80-20% train/test ratio. Due to the relatively small size of some datasets, we decided to use sites 3, 5 & 6 entirely for training and kept the patients from sites 4 & 7 as held-out (unseen) test sets to evaluate the model’s generalization performance. The model was trained on a total of 281 T2w images and tested on 75 images. The ground truth masks of intramedullary lesions appearing as T2w signal abnormalities were manually annotated by expert raters at individual sites [14]. The SC masks were automatically segmented using the `sct_deepseg_sc` [6] algorithm and manually corrected when necessary.

### 2.2 SCIsegV2

We used nnUNet [10] as the backbone architecture for the SCI lesion segmentation model. The continuing dominance of nnUNet [10,9] across several open-source challenges has shown that a well-tuned convolutional neural network (CNN) architecture is robust and continues to achieve state-of-the-art results over novel (and more sophisticated) transformer-based architectures in dense pixel prediction tasks such as image segmentation.

Similar to the recent work building upon the nnUNet framework [21,11], we experimented with its easy-to-tweak trainers for developing SCIsegV2. Specifically, we used: (i) `nnUNetTrainer`, the default model, and (ii) `nnUNetTrainerDA5`, the model applying aggressive data augmentation. The augmentation methods in

the standard `nnUNetTrainer` include random rotation, scaling, mirroring, Gaussian noise addition, Gaussian blurring, adjusting image brightness and contrast, low-resolution simulation, and Gamma transformation. In addition to the standard augmentations, `nnUNetTrainerDA5` applies additional transforms such as random patch replacement with mean values, sharpening, median filter, gamma correction, and additive intensity gradients. We note that even though the training data is a collection of heterogeneous datasets (acute, chronic traumatic and non-traumatic SCI) from 7 sites, we employed stronger data augmentation to improve generalization across various types of lesions.

The wide spectrum of lesion intensities in different SCI etiologies makes lesion segmentation an extremely challenging task. For instance, lesions in acute SCI are mildly T2w hyperintense and chronic lesions are bright T2w hyperintense (Figure 1), although typically surrounded by metallic implants causing heavy interference [5]. Therefore, we compared two different training strategies for lesion segmentation: (i) given just the T2w image as the input, the model is trained to segment both the SC and lesions in hierarchical ordering, and (ii) assuming the availability of SC segmentation mask, the model is trained to segment only the lesions, given a 2-channel input consisting of the T2w image concatenated with the SC mask. While the first strategy attempts to implicitly guide the model towards the SC for lesion segmentation, the latter provides an explicit guidance in the form of the input channel.

### 2.3 Automatic Quantification of Tissue Bridges

The manual measurement of tissue bridges is performed on a single midsagittal slice of a volumetric (3D) T2w MRI image [8,24,17,19,20,16,23,18] (Figure 2A). The midsagittal slice is defined as the middle slice of all slices where the SC is visible (Figure 2B). Ventral and dorsal tissue bridges are quantified as the width of spared tissue at the minimum distance from the intramedullary lesion edge to the boundary between the SC and cerebrospinal fluid (Figure 2C).

To automate the measurement of tissue bridges, we propose a method that computes ventral and dorsal tissue bridges utilizing the lesion and SC segmentation masks. To compensate for different neck positions and, consequently, different SC curvatures, we use angle correction, which adjusts the tissue bridge widths with respect to the SC centerline [7]. The method computes tissue bridges from all sagittal slices containing the lesion, allowing quantification of not only midsagittal but parasagittal tissue bridges as well. For the purpose of this study (and to compare against existing manual measurements based on midsagittal tissue bridges), we considered only the midsagittal slice for the automatic measurement of the tissue bridges.

### 2.4 Experiments

We divided our experiments into 3 categories to investigate the effects of input types, data augmentation strategies and SCI etiology-specific models. All images

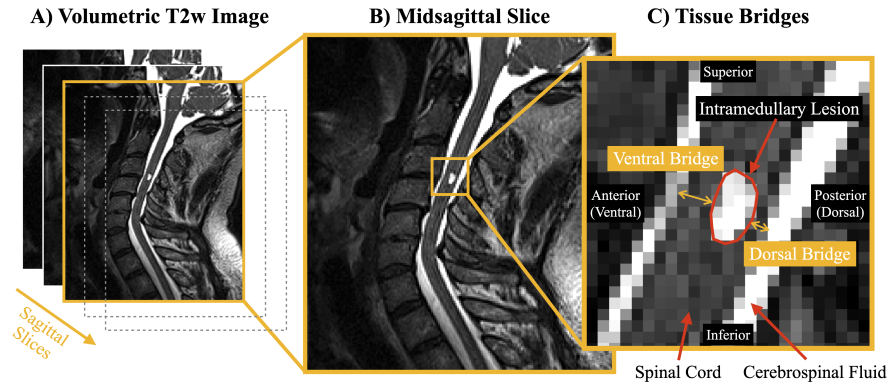


**Fig. 2.** Illustration of tissue bridges. A) Volumetric T2w image of a spinal cord injury (SCI) with chronic intramedullary lesion. B) Midsagittal slice used to compute the tissue bridges. C) Ventral and dorsal tissue bridges are defined as the width of spared tissue at the minimum distance from the intramedullary lesion edge to the boundary between the SC and cerebrospinal fluid.

were preprocessed with right-left, posterior-anterior, inferior-superior (RPI) orientation, resampled to a common resolution ( $0.92 \times 0.68 \times 0.92 \text{ mm}^3$ , which is the median of all image resolutions in the training set) and intensity-normalized using Z-score normalization. The model was trained for 1000 epochs with 5-fold cross-validation, using a batch size of 2 and the stochastic gradient descent optimizer with a polynomial learning rate scheduler.

**Inputs** We trained 2 different models: (i) a model that segments *both* the SC and lesions given just the T2w image as input (referred to as *single*), and (ii) a model that segments *only* the lesion given a 2-channel input consisting of T2w image and the SC segmentation (referred to as *multi*). As briefly discussed in Section 2.2, this experiment is to understand whether providing additional (localization) context in the form of SC segmentation as input would improve the lesion segmentation performance.

**Data augmentation** Given the increasing literature towards unrealistic transformations leading to better test-time performance [2], we compared 2 models with and without aggressive data augmentation to understand which model leads to better generalization on external test sets with acute preoperative SCI images. These are referred to as *defaultDA* and *aggressiveDA*, respectively.

**SCI Etiology-specific models** This crucial experiment will provide insight into the initial hypothesis, asking whether a comprehensive SCI model is achievable. Toward this end, we compared our *SCIsegV2* model trained on all 7 sites against etiology-specific models individually trained on non-traumatic SCI and acute preoperative SCI data, respectively.

**SCIseg** We also evaluate our model against SCIseg [14] which was trained on data from three sites comprising traumatic and ischemic SCI lesions. The model used a three-phase training strategy involving active learning and is available in SCT. Details about the training strategy can be found in [14].

**Tissue Bridges** To validate the automatic measurements of the tissue bridges, we compared the method against manual and semi-automatic techniques in 15 individuals with traumatic SCI from site 1. Specifically, we compared the following: (1) **manual** — manual measurement of tissue bridges on manually segmented intramedullary lesions, (2) **semi-automatic** — automatic measurement of the tissue bridges using the proposed method on manually segmented intramedullary lesions, and (3) **fully-automatic** — automatic measurement of tissue bridges using SCIsegV2 predictions. Statistical analysis was performed using the SciPy v1.10.0. The distribution of the data was assessed with the D’Agostino and Pearson normality test. Subsequently, the Kruskal-Wallis H-test was performed to compare the methods independently for ventral and dorsal bridges.

**Evaluation Metrics** We used MetricsReloaded [12] and contributed to its development by adding lesion-wise metrics, specifically, lesion-wise sensitivity, positive predictive value, and  $F_1$ -score in addition to the existing metrics.

### 3 Results

Figure 3 shows the test Dice scores averaged across 5 folds for all models described in Section 2.4. Starting with the etiology-specific models, we observed that the model trained only on acute preoperative (**AcuteSCI**) data does not perform well on sites 1 and 2 containing non-traumatic and traumatic SCI data. While it performs relatively better on test sets from unseen sites (sites 4 and 7), it does not outperform the **SCIsegV2** models. Likewise, the model trained only on non-traumatic SCI data (**DCM**) performs well on a similar test set but fails in generalizing to acute preoperative SCI of sites 4 and 7.

Since **SCIsegV1** [14] was trained on a dataset of 3 sites predominantly consisting of traumatic SCI, it outperforms **SCIsegV2** models in sites 1 and 2. However, we observed that even **SCIsegV1** performs poorly on sites 4 and 7 suggesting that the segmentation of acute preoperative SCI lesions is extremely challenging. Within **SCIsegV2** models, we noted that training with aggressive data augmentation only results in marginal improvements in lesion segmentation performance. However, concatenating the SC segmentation as a second channel along with the input image (resulting in a 2-channel input) showed considerable improvements, especially in acute preoperative images, compared to a single-channel input with just the T2w image.

In Table 1, we present a quantitative comparison of different models using lesion-wise metrics. We noticed that the models’ performance depends heavily on the specific SCI phases and etiologies. Except for site 1 (traumatic SCI), **SCIsegV2** outperforms **SCIsegV1** in all other sites. Comparing within the **SCIsegV2**

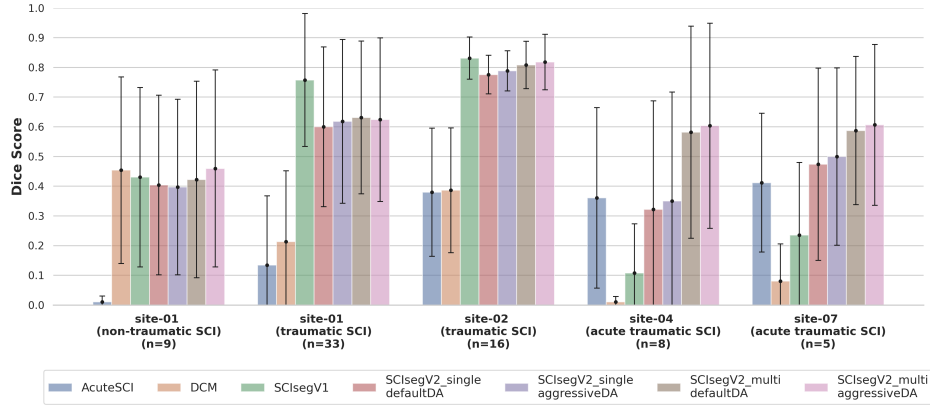


**Fig. 3.** Comparison of Dice scores for different SCI models. Each bar plot shows the test Dice scores averaged across 5 folds (the error bar represents the standard deviation).

**Table 1.** Comparison of lesion-wise metrics for `SCIsegV1` and various `SCIsegV2` models (with `aggressiveDA`) across the 5 testing sites. Metrics correspond to lesion-wise positive predictive value (PPVL), sensitivity (SensL) and  $F_1$ -score; higher the value the better ( $\uparrow$ ). For a given site, bold values in each column represent the best model.

Model	Metric	Test Sites				
		site-01 (DCM)	site-01 (tSCI)	site-02 (tSCI)	site-04 (acuteSCI)	site-07 (acuteSCI)
SCIsegV1	( $\uparrow$ ) PPVL	<b>0.63</b> $\pm$ <b>0.43</b>	<b>0.81</b> $\pm$ <b>0.31</b>	0.95 $\pm$ 0.14	0.37 $\pm$ 0.50	0.62 $\pm$ 0.50
	( $\uparrow$ ) SensL	0.78 $\pm$ 0.44	<b>0.95</b> $\pm$ <b>0.16</b>	0.97 $\pm$ 0.12	0.55 $\pm$ 0.49	0.72 $\pm$ 0.49
	( $\uparrow$ ) $F_1$ ScoreL	0.67 $\pm$ 0.42	<b>0.84</b> $\pm$ <b>0.26</b>	0.95 $\pm$ 0.12	0.35 $\pm$ 0.47	0.64 $\pm$ 0.49
SCIsegV2 single	( $\uparrow$ ) PPVL	0.55 $\pm$ 0.45	0.73 $\pm$ 0.33	<b>0.96</b> $\pm$ <b>0.13</b>	0.55 $\pm$ 0.50	<b>0.78</b> $\pm$ <b>0.36</b>
	( $\uparrow$ ) SensL	0.68 $\pm$ 0.49	0.91 $\pm$ 0.24	<b>0.97</b> $\pm$ <b>0.12</b>	0.63 $\pm$ 0.48	<b>0.84</b> $\pm$ <b>0.36</b>
	( $\uparrow$ ) $F_1$ ScoreL	0.59 $\pm$ 0.45	0.77 $\pm$ 0.28	<b>0.95</b> $\pm$ <b>0.12</b>	0.53 $\pm$ 0.49	<b>0.80</b> $\pm$ <b>0.35</b>
SCIsegV2 multi	( $\uparrow$ ) PPVL	0.61 $\pm$ 0.41	0.70 $\pm$ 0.36	0.90 $\pm$ 0.20	<b>0.75</b> $\pm$ <b>0.39</b>	0.54 $\pm$ 0.41
	( $\uparrow$ ) SensL	<b>0.80</b> $\pm$ <b>0.42</b>	0.90 $\pm$ 0.26	0.97 $\pm$ 0.12	<b>0.90</b> $\pm$ <b>0.25</b>	0.80 $\pm$ 0.42
	( $\uparrow$ ) $F_1$ ScoreL	<b>0.67</b> $\pm$ <b>0.40</b>	0.74 $\pm$ 0.32	0.91 $\pm$ 0.15	<b>0.75</b> $\pm$ <b>0.37</b>	0.60 $\pm$ 0.40

models, one of downsides of the `multi`-models, despite achieving higher Dice scores (Figure 3), is its dependency on the SC masks as input.

Table 2 shows the comparison of the midsagittal tissue bridges obtained using different methods (manual vs semi-automatic vs fully-automatic; see Section 2.4 for details) for 15 patients with traumatic SCI from site 1. For the fully-automatic technique, we used the `SCIsegV2_single_aggressiveDA` model to obtain the lesion segmentations. There was *no* statistically significant ( $p > .05$ ) difference between the bridges computed using different methods.

**Table 2.** Comparison of *ventral* and *dorsal* midsagittal tissue bridges between manual, semi-automatic, and automatic measurements. Values are reported in millimetres.

ID	Manual Lesions & Manual Measurements		Manual Lesions & Automatic Measurements		SCIsegV2 Predictions & Automatic Measurements	
	Ventral	Dorsal	Ventral	Dorsal	Ventral	Dorsal
	sub-zh101	0	2.65	0	2.39	0.34
sub-zh102	2.10	0.83	2.25	0	2.27	0.67
sub-zh104	0	0	0.54	0	0.55	0
sub-zh105	2.70	0	2.38	0.60	2.99	0
sub-zh106	0	0	0	0	0	0
sub-zh107	0	0.76	0	0.67	0	0.65
sub-zh108	1.32	0.52	1.96	0.66	2.03	0.68
sub-zh109	1.13	1.03	0.71	0	1.08	0.73
sub-zh110	0	0.99	0	0	0	0.39
sub-zh112	3.01	0.36	1.70	0.44	2.64	0.44
sub-zh114	0	0	0	0.38	0	0
sub-zh115	0	0	0	2.12	0	0.42
sub-zh116	3.12	0.50	2.38	0	2.49	0.80
sub-zh118	0.40	0	0	0	0	0
sub-zh119	2.93	2.98	1.04	0.50	1.48	0.95

## 4 Discussion

In this work, we proposed **SCIsegV2**, a DL-based universal tool for the segmentation of intramedullary lesions across different SCI etiologies and phases. We also automated the calculation of midsagittal tissue bridges, a metric representing spared spinal tissue adjacent to the lesion. This metric is relevant as it is associated with functional recovery in individuals with SCI. Both **SCIsegV2** and the automatic tissue bridges computation are open-source and available in Spinal Cord Toolbox (v6.4 and above) via the `sct_deepseg -task seg_sc_lesion_t2w_sci` and `sct_analyze_lesion` functions, respectively.

The heterogeneity in the appearance of intramedullary lesions across different SCI phases (acute, sub-acute, chronic) and etiologies (traumatic SCI, ischemic SCI, DCM) makes lesion segmentation extremely challenging, even for trained radiologists. Relatively low prevalence of traumatic SCI and the need for early surgical intervention [1] result in a low number of preoperative MRI scans, which adds to the difficulty in training a robust automatic segmentation model, that performs well on "real world" clinical data across multiple sites. Moreover, MRI scans of individuals with chronic SCI frequently exhibit image distortions caused by metallic implants, further complicating the segmentation process.

As a way of simplifying the lesion segmentation problem, using the SC mask to explicitly guide the model towards the cord showed improved results on certain etiologies. However, it introduced a dependency on the SC mask to be concatenated to the input image, preventing a smooth transition from the model's automatic predictions to the computation of tissue bridges, which requires both the cord and lesion masks. In contrast, the **SCIsegV2\_single** model capable of segmenting both SC and lesions has a higher utility as it is also applicable in scenarios where SC masks are unavailable. Lastly, as the lesion appearance



varies substantially across different SCI types, universal models like **SCIsegV2** learn the differences in lesion distributions across etiologies and even outperform etiology-specific models while showing good generalization across sites.

**Limitations and Future Work** One limitation of the model is its higher sensitivity to traumatic SCI lesions, as approximately ( $\sim 70\%$ ) of our dataset consists of this population. This skew is due to the relatively low availability of acute preoperative SCI scans. Acquiring additional data in SCI is generally challenging, but is possible with the help of ongoing clinical trials and consortiums for creating large databases for SCI research [15,3]. While this work used a relatively small and unbalanced cohort, we presented a preliminary proof-of-concept toward a universal tool for SCI lesion segmentation. The current literature only quantifies tissue bridges manually, from a single *midsagittal* slice. However, as lesions are 3D blob-like objects, the midsagittal slice might not necessarily contain the largest portions of the lesion and does not consider parasagittally running fiber tracts. Therefore, combining both *parasagittal* and *midsagittal* slices could provide a comprehensive evaluation of the width of the spared tissue bridges.

**Prospect of application** Automatic segmentation of the lesions and spinal cord could mitigate the bottleneck and inter-rater variability associated with manual annotations. Automating the measurements of tissue bridges could provide an objective, unbiased way in guiding rehabilitation decision making and stratifying patients into homogeneous subgroups of recovery in clinical trials.

**Acknowledgments.** We thank Mathieu Guay-Paquet and Joshua Newton for their assistance with the management of the datasets and the implementation of the algorithm to SCT. We thank Maxime Bouthillier for the help with manual annotations. We thank Dr. Serge Rossignol and the Multidisciplinary Team on Locomotor Rehabilitation (Regenerative Medicine and Nanomedicine, CIHR), and all the patients. The authors would also like to thank the RHSCIR participants and network, including all the participating local RHSCIR sites: Vancouver General Hospital, Foothills Hospital, Royal University Hospital, Toronto Western Hospital, St. Michael’s Hospital, Sunnybrook Health Sciences Centre, Hamilton General Hospital, The Ottawa Hospital Civic Campus, Hôpital de l’Enfant Jésus, Hôpital du Sacre Coeur de Montréal, QEII Health Sciences Centre, Saint John Regional Hospital.

Funded by the Canada Research Chair in Quantitative Magnetic Resonance Imaging [CRC-2020-00179], the Canadian Institute of Health Research [PJT-190258], the Canada Foundation for Innovation [32454, 34824], the Fonds de Recherche du Québec - Santé [322736, 324636], the Natural Sciences and Engineering Research Council of Canada [RGPIN-2019-07244], the Canada First Research Excellence Fund (IVADO and TransMedTech), the Courtois NeuroMod project, the Quebec BioImaging Network [5886, 35450], INSPIRED (Spinal Research, UK; Wings for Life, Austria; Craig H. Neilsen Foundation, USA), Mila - Tech Transfer Funding Program, the Association Française contre les Myopathies (AFM), the Institut pour la Recherche sur la Moelle épinière et l’Encéphale (IRME), the National Institutes of Health Eunice Kennedy Shriver National Institute of Child Health and Development (R03HD094577). ACS is supported by the National Institutes of Health – K01HD106928 and R01NS128478 and the Boettcher Foundation’s Webb-Waring Biomedical Research Program. KAW is supported by the National Institutes of Health – K23NS104211, L30NS108301,

R01NS128478. The Rick Hansen Spinal Cord Injury Registry and this work are supported by funding from the Praxis Spinal Cord Institute through the Government of Canada and the Province of British Columbia. For more information about RHSCIR(9), please visit [www.praxisinstitute.org](http://www.praxisinstitute.org). JV received funding from the European Union’s Horizon Europe research and innovation programme under the Marie Skłodowska-Curie grant agreement No 101107932 and is supported by the Ministry of Health of the Czech Republic, grant nr. NU22-04-00024. ENK is supported by the Fonds de Recherche du Québec Nature and Technologie (FRQNT) Doctoral Training Scholarship. The authors thank Digital Research Alliance of Canada for the compute resources used in this work.

**Disclosure of Interests.** The authors have no competing interests to declare that are relevant to the content of this article.

## References

1. Ahuja, C.S., Wilson, J.R., Nori, S., Kotter, M.R.N., Druschel, C., Curt, A., Fehlings, M.G.: Traumatic spinal cord injury. *Nat. Rev. Dis. Primers* **3**(1) (Apr 2017)
2. Billot, B., Greve, D.N., Puonti, O., Thielscher, A., Van Leemput, K., Fischl, B., Dalca, A.V., Iglesias, J.E.: Synthseg: Segmentation of brain MRI scans of any contrast and resolution without retraining. *Medical Image Analysis* **86**, 102789 (2023)
3. Birkhäuser, V., et al.: Tasci—transcutaneous tibial nerve stimulation in patients with acute spinal cord injury to prevent neurogenic detrusor overactivity: protocol for a nationwide, randomised, sham-controlled, double-blind clinical trial. *BMJ Open* **10**(8) (2020)
4. David, G., Mohammadi, S., Martin, A.R., Cohen-Adad, J., Weiskopf, N., Thompson, A., Freund, P.: Traumatic and nontraumatic spinal cord injury: pathological insights from neuroimaging. *Nat. Rev. Neurol.* **15**(12), 718–731 (Dec 2019)
5. Freund, P., Seif, M., Weiskopf, N., Friston, K., Fehlings, M.G., Thompson, A.J., Curt, A.: MRI in traumatic spinal cord injury: from clinical assessment to neuroimaging biomarkers. *Lancet Neurol.* **18**(12), 1123–1135 (2019)
6. Gros, C., De Leener, B., Badji, A., Maranzano, J., Eden, D., Dupont, S.M., Talbott, J., Zhuoquiong, R., Liu, Y., Granberg, T., et al.: Automatic segmentation of the spinal cord and intramedullary multiple sclerosis lesions with convolutional neural networks. *Neuroimage* **184**, 901–915 (2019)
7. Gros, C., De Leener, B., Dupont, S.M., Martin, A.R., Fehlings, M.G., Bakshi, R., Tummala, S., Auclair, V., McLaren, D.G., Callot, V., Cohen-Adad, J., Sdika, M.: Automatic spinal cord localization, robust to MRI contrasts using global curve optimization. *Med. Image Anal.* **44**, 215–227 (Feb 2018)
8. Huber, E., Lachappelle, P., Sutter, R., Curt, A., Freund, P.: Are midsagittal tissue bridges predictive of outcome after cervical spinal cord injury? *Ann. Neurol.* **81**(5), 740–748 (May 2017)
9. Isensee, F., Wald, T., Ulrich, C., Baumgartner, M., Roy, S., Maier-Hein, K., Jaeger, P.F.: nnu-net revisited: A call for rigorous validation in 3d medical image segmentation (2024)
10. Isensee, F., et al.: nnu-net: a self-configuring method for deep learning-based biomedical image segmentation. *Nature methods* **18**(2), 203–211 (February 2021)

11. Ma, J., Li, F., Wang, B.: U-mamba: Enhancing long-range dependency for biomedical image segmentation. ArXiv [abs/2401.04722](https://arxiv.org/abs/2401.04722) (2024)
12. Maier-Hein, L., Reinke, A., Godau, P., Tizabi, M.D., Buettner, F., Christodoulou, E., Glocker, B., Isensee, F., Kleesiek, J., Kozubek, M., et al.: Metrics reloaded: recommendations for image analysis validation. *Nature methods* pp. 1–18 (2024)
13. McCoy, D.B., et al.: Convolutional neural Network–Based automated segmentation of the spinal cord and contusion injury: Deep learning biomarker correlates of motor impairment in acute spinal cord injury. *AJNR Am. J. Neuroradiol.* **40**(4), 737–744 (Mar 2019)
14. Naga Karthik, E., Valosek, J., Smith, A.C., Pfyffer, D., Schading-Sassenhausen, S., Farner, L., Weber, K.A., Freund, P., Cohen-Adad, J.: Sciseg: Automatic segmentation of t2-weighted intramedullary lesions in spinal cord injury. *medRxiv* (2024)
15. Noonan, V.K., Kwon, B.K., Soril, L., Fehlings, M.G., Hurlbert, R.J., Townson, A., Johnson, M., Dvorak, M.F.: The rick hansen spinal cord injury registry (rhscir): a national patient-registry. *Spinal Cord* **50**(1), 22–27 (Nov 2011)
16. O’Dell, D.R., Weber, K.A., Berliner, J.C., Elliott, J.M., Connor, J.R., Cummins, D.P., Heller, K.A., Hubert, J.S., Kates, M.J., Mendoza, K.R., Smith, A.C.: Midsagittal tissue bridges are associated with walking ability in incomplete spinal cord injury: A magnetic resonance imaging case series. *J. Spinal Cord Med.* **43**(2), 268–271 (Mar 2020)
17. Pfyffer, D., Huber, E., Sutter, R., Curt, A., Freund, P.: Tissue bridges predict recovery after traumatic and ischemic thoracic spinal cord injury. *Neurology* **93**(16), e1550–e1560 (Oct 2019)
18. Pfyffer, D., Smith, A.C., Weber, K.A., Grillhiesl, A., Mach, O., Draganich, C., Berliner, J.C., Tefertiller, C., Leister, I., Maier, D., Schwab, J.M., Thompson, A., Curt, A., Freund, P.: Prognostic value of tissue bridges in cervical spinal cord injury: a longitudinal, multicentre, retrospective cohort study. *The Lancet Neurology* (2024)
19. Pfyffer, D., Vallotton, K., Curt, A., Freund, P.: Tissue bridges predict neuropathic pain emergence after spinal cord injury. *J. Neurol. Neurosurg. Psychiatry* **91**(10), 1111–1117 (Oct 2020)
20. Pfyffer, D., Vallotton, K., Curt, A., Freund, P.: Predictive value of midsagittal tissue bridges on functional recovery after spinal cord injury. *Neurorehabil. Neural Repair* **35**(1), 33–43 (Jan 2021)
21. Roy, S., Koehler, G., Ulrich, C., Baumgartner, M., Petersen, J., Isensee, F., Jaeger, P.F., Maier-Hein, K.H.: Mednext: Transformer-driven scaling of convnets for medical image segmentation. In: *International Conference on Medical Image Computing and Computer-Assisted Intervention* (2023)
22. Seif, M., David, G., Huber, E., Vallotton, K., Curt, A., Freund, P.: Cervical cord neurodegeneration in traumatic and Non-Traumatic spinal cord injury. *J. Neurotrauma* **37**(6), 860–867 (Mar 2020)
23. Smith, A.C., O’Dell, D.R., Thornton, W.A., Dungan, D., Robinson, E., Thaker, A., Gisbert, R., Weber, 2nd, K.A., Berliner, J.C., Albin, S.R.: Spinal cord tissue bridges validation study: Predictive relationships with sensory scores following cervical spinal cord injury. *Top. Spinal Cord Inj. Rehabil.* **28**(2), 111–115 (2022)
24. Vallotton, K., Huber, E., Sutter, R., Curt, A., Hupp, M., Freund, P.: Width and neurophysiologic properties of tissue bridges predict recovery after cervical injury. *Neurology* **92**(24), e2793–e2802 (Jun 2019)